Volume 14, Issue 3, 142422 (1-16)

Iranian Journal of Catalysis (IJC)

https://doi.org/10.57647/j.ijc.2024.1403.22

Fe_3O_4@C–SO_3H Novel, green and recyclable acid catalysts for the synthesis of 2-amino-4*H*-chromene derivatives

Raju Shekhanavar[1], Santosh Y. Khatavi[2], Aravind D. Kamath[1], Kantharaju Kamanna[1,*]

[1]*Department of Chemistry, Peptide, and Medicinal Chemistry Research Laboratory, Rani Channamma University, Belagavi, Karnataka, India.*
[2]*Centre for Nano and Soft Matter Sciences, Bangalore, India.*

Corresponding author: kk@rcub.ac.in

Original Research

Received:
28 February 2024
Revised:
21 April 2024
Accepted:
11 August 2024
Published online:
17 September 2024

Abstract:

A novel iron oxide nanoparticle (Fe_3O_4@C–SO_3H) fabricated with carbon and sulfonic acid was prepared using the concept of green chemistry protocol. The usage of agro-waste extract for core-shell Fe_3O_4 preparation and its biochar powder as a carbon source for the fabrication of the catalyst was the dual benefit. This prepared catalyst was employed for the synthesis of 4*H*-chromene derivative *via* a three-component one-pot reaction of resorcinol, aryl aldehyde, and malononitrile in ethanol under microwave irradiation. The method was found to be nontoxic, inexpensive, faster, and simple work-up with greener solvent, and gave excellent product isolation with about 91 % yield in 4 min microwave irradiation in the presence of 25 mg catalyst. The catalyst could be recovered after the reaction by an external magnet and reused for up to four runs without any considerable loss in its catalytic activity. The prepared catalyst was characterized by FT-IR, and prominent bands were observed for surface functionalization. The XRD data revealed prominent peaks for the formation of Fe_3O_4@C–SO_3H, and the results are comparable with the reported literature; the VSM data gives a clear idea about the magnetic nature of the catalyst and respective surface-modified core shells, the surface morphology, and the required elements present are confirmed by FE-SEM and EDX. TGA admits that the thermal stability of the catalyst is up to 600 °C under a nitrogen atmosphere. The ^{1}H- & ^{13}C-NMR and LC-MS analysis are explored for the analysis of the formation of final 2-amino-4*H*-chromene derivatives. Further antimicrobial activities of the selected compounds were performed, and the results are promising and comparable with the reference.

Keywords: 2-Amino-4*H*-chromene; Antimicrobial activity; Recyclable catalyst; Green method

1. Introduction

Numerous organic reactions have been catalyzed with homogeneous and heterogeneous catalysts [1–4]. In the case of homogeneous catalysts, the researchers have encountered disadvantages like separation, recyclability, harsh reaction conditions, and low stability [5–7]. However, the heterogeneous catalysts exhibit advantages like high stability [8], catalyst recovery, eco-friendliness, and inexpensiveness [9–11]. Nanoparticles (NPs) have emerged as one of the best choices of recent materials for the development of heterogeneous catalysts due to their additional properties like increased surface area, easy preparation, and size [12]. Their increased surface area to volume ratio leads to high dispersion and availability of more catalytic activity sites, making the reactant interactions more effective [13–17]. Additionally, these catalysts can be easily separated

from the reaction mixture and reused after the reaction. Hence, NPs have emerged as a choice of both homogeneous and heterogeneous catalysts [18]. In recent years, magnetic nanoparticles (MNPs) have taken considerable attention from researchers in the heterogeneous catalysts development [19] due to their unique properties of high dispersion rate, high activity [20], and easy separation by using an external magnet. Bare Fe_3O_4 NPs are vulnerable to agglomeration easily, making their surface less active. Consequently, researchers have developed fabrication on the surface of the MNPs to overcome some of these vulnerable properties [21]. In addition, the modification of the core-shell to different inorganic and organic shells has resulted in a wide range of heterogeneous acid/base catalysts being employed in various organic transformations [22–27]. Carbon is one of the superior protecting shells, which is stable to the action of acid-base, high pressure, and temperature [28–30]. The presence of C=O and O–H functional groups on the carbon simplifies the attachment of another catalytic functional group on the carbon surface, while the magnetic properties of the core give easy separation of the catalysts by an external magnet. Multicomponent reactions (MCRs), where three or more reactants are reacted in a single pot to give a complex heterocycle structure, are a promising route for the chemists for the synthesis [31]. The use of green solvent for the MCRs [32] is advantageous to the chemistry [33]. MCRs have emerged as superior routes in the construction of complex molecules due to their faster reaction rate [34–36], atom economy [37], simplicity, inexpensiveness [38–40], and high isolated yield. This has attracted chemists to consider MCRs for the synthesis of valuable bioactive heterocycle molecules [41]. 4*H*-Chromene, also named Benzo[b]dihydro-pyrone, is an important class of synthetic as well as naturally abundant oxygen-containing heterocyclic skeleton [42]. Its derivatives show various biological activities such as antimicrobial, anticancer, antiproliferation, and antimutagenic activities [43]. Hence, chemists are very much interested to construct various 4*H*-chromene derivatives, especially employing heterogeneous catalysts [44]. Numerous reported synthetic routes for the synthesis of chromene derivatives by the condensation reaction of resorcinol, aryl aldehyde, and malononitrile in the presence of catalysts such as Cu@MNPs [45], Ionic liquids [46], $Ca(OH)_2$ [47], $(\gamma\text{-}Fe_2O_3\text{-Im-Py})_2WO_4$ [48], $SiO_2@Fe_3O_4$ [49], Potassium phthalimide [50], Na_2CO_3 [51], potassium phthalimide-*N*-oxyl (POPINO) [52], Pd@GO [53], hexadecyltrimethyl ammonium bromide (HTMAB) [54], Triazine based porous organic polymer [55], NaBr [56], Tungstic acid functionalized mesoporous SBA-15 [57], Functionalization of magnetic nanoparticles by creatine [58], $Cu(OAc)_2$[59], K_2CO_3/cyanuric acid catalyzed [60], Ionic liquid [61], Silica gel supported polyamine [62], and p-Dimethylaminopyridine (DMAP) [63]. These homogeneous and heterogeneous catalysts involved in the synthesis suffer from some disadvantages, such as toxicity, lengthy procedures, low yield isolation, harsh conditions, and tedious catalyst isolation. To overcome some of these demerits, synthetic methods that allow the easy separation of the catalysts by an external magnet have emerged as a superior choice, and their application in organic reactions is well documented [64]. In this work, we report for the first time the preparation of a core shell and fabrication of magnetic nanoparticles of Fe_3O_4 using the agro-waste lemon peel. The developed method has dual benefits, where the lemon peel ash extract provides a green medium for the preparation of the core Fe_3O_4 starting from $FeCl_3$ and $FeSO_4$, and the left-over ash powder can be employed for the carbon coating on prepared Fe_3O_4. Further, it is functionalized by chlorosulfonic acid to sulfonic acid to give a $Fe_3O_4@C-SO_3H$ heterogeneous catalyst. The one-pot MCRs of resorcinol, aryl aldehyde, and malononitrile in ethanol under MWI to yield 4*H*-chromene derivatives catalyzed by $Fe_3O_4@C-SO_3H$ demonstrates an efficient method and recyclability. The catalyst shows efficient catalysis for the reaction and can be easily recovered by an external magnet.

2. Experimental

The required chemicals for this work were purchased from Avra and sd-fine chemicals and used directly as received without further purification. The custom-made microwave reactor model BM-12574-066 was used for the reaction. FT-IR spectra were collected by the KBr disk method using a Perkin Elmer Spectrum GX spectrometer. The XRD data was recorded using PANalytical (X-pert PRO). The surface morphology and elemental mapping, EDS, was analyzed by TESCAN and Bruker [MIRA 3 (FESEM) and Quantax 200 (EDS), Evactron XEI (plasma cleaner)]. TG-DTA was recorded by NETZSCH (STA 2000). The magnetic properties were determined by a Vibrating Sample Magnetometer (VSM). ^{1}H- and ^{13}C-NMR were recorded on a 400 MHz Bruker spectrometer using TMS as an internal standard and solvent $CDCl_3$ or DMSO-d_6. Waters: SynaptG2 was used for LC-MS recording. The melting points of the derivatives prepared were determined using a capillary and are uncorrected.

2.1 Preparation of Water Extract of Lemon Fruit Shell (WELFSA)

The ash medium was extracted by a previously reported procedure [65]. Briefly, lemon peel collected from the local market was washed with water and dried in open sunlight. The dried peel was burnt aerobic environment on Bunsen flame rather than the muffle furnace, this will helps to form the oxides and carbonates of respective ions like K, Ca, Na present in the lemon peel and causes basic nature to the extract. 10 g of the resultant ash was weighed and suspended in 100 mL of double distilled water (dd water) and stirred for 1 h at room temperature. The mixture was filtered, and the brown-colored filtrate was named Water Extract of Lemon Fruit Shell (WELFSA).

2.2 Preparation of Fe_3O_4 using WELFSA

3.0 g of $FeSO_4 \cdot 7H_2O$ and 3.2 g of $FeCl_3 \cdot 6H_2O$ were weighed and taken in a 250 mL beaker, dissolved in 50 mL of dd water, and then 10 mL of WELFSA was added. The mixture was heated to 90 °C for about 45 min with stirring, and then cooled to room temperature, added NH_4OH drop-

wise till the formation of black precipitate stopped, and then it was allowed to settle down. The black precipitate was held by an external magnet and washed several times with dd water, followed by ethanol. The resultant residue was calcinated in a muffle furnace at 700 °C for about 5 h, stored in an air-tight container, and kept in a desiccator until further use.

2.3 Synthesis of Fe_3O_4@C

10 g of lemon peel ash residue after the extraction of the filtrate was taken in a 250 mL beaker, and 100 mL dd water was added and stirred at room temperature for 1 h. To this, 3 g of the above-prepared Fe_3O_4 NPs were added, and the resultant mixture was dispersed in an ultrasonic bath for about 30 min. Then the whole mixture was transferred to a 100 mL Teflon-lined stainless-steel autoclave and kept at 180 °C in an oven for 10 h. The carbon intermediate was magnetically attracted, and washed with dd water, and ethanol thoroughly, and dried at 70 °C in an oven under vacuum for 10 h to give free-flowing powder, and was denoted as Fe_3O_4@C.

2.4 Synthesis of Fe_3O_4@C–SO_3H

1.5 g of Fe_3O_4@C was weighed in a 100 mL beaker and con. H_2SO_4 (9 mL) was added to this slowly and stirred at room temperature. After stirring for 45 min, the resultant mixture was transferred into a 100 mL sealed Teflon-lined autoclave and kept at 160 °C in an oven for 12 h. After cooling to room temperature, the resulting black solid was held by an external magnet and washed with hot dd water and ethanol 2–3 times to remove any physically adsorbed species until the sulfate ions were no longer detected. Then, it was dried at 60 °C in an oven under vacuum for 12 h, and the catalyst was denoted as Fe_3O_4@C–SO_3H.

2.5 Solid acid titration

The acid-functionalized sulfonic acid group (Fe_3O_4@C–SO_3H) was titrated by a common acid-base titration method. Briefly, 30 mg of the acid catalyst was taken in 50 mL of (0.01 M) NaOH in a conical flask (100 mL) kept at room temperature for about 3 h. Then, the catalyst was filtered by a magnetic rotator and washed with dd water (5 mL) two times. After that, the filtrate was titrated to neutrality using a 0.01 M HCl using phenolphthalein indicator. The total acid group on Fe_3O_4@C MNPs, and in turn, the number of carbon functionalized sulphonic acid (C–SO_3H), was found to be 0.47 mmol/g.

2.6 General procedure for the synthesis of 2-amino-4*H*-chromene derivatives under microwave irradiation

The targeted 2-amino-4*H*-chromene derivatives are synthesized by using the custom-made microwave reactor having a stirring, reflux, and power control facility. The reactants aldehyde, malononitrile, and resorcinol were taken into the round-bottomed flask, and then the optimized amount of catalyst, i.e., 25 mg, was added. Then, the magnetic bead was inserted to avoid bumping the reaction mixture, and for stirring purposes, the reaction mixture was irradiated with a microwave for completion of the reaction. The reaction completion was monitored by thin-layer chromatography; the catalyst was separated by using a strong magnet, and the product was isolated (the detailed synthetic procedure is explained in Scheme 1).

2.7 General procedure for antimicrobial assay

The antimicrobial activities of selected synthesized 2-amino-4*H*-chromene derivatives were evaluated by standard disc diffusion method. The antimicrobial inhibition assay was carried out *in vitro* using agar media at 37 °C incubation using gram positive and gram negative bacteria, fungi and compared with known antimicrobial agents.

2.8 Spectral data of some selected derivatives

2-Amino-3-cyano-7-hydroxy-4-phenyl-4*H*-chromene (4a): Solid; Light yellow; FT-IR: 3495.88, 3425.59 (NH_2), 3334.61 (OH), 2189.75 (CN), 1650.17 (C=C), ^{1}H NMR(DMSO-d_6): (δ ppm) 4.60 (CH, s, 1H), 6.41 (CH, s, 1H), 6.47 (CH, d, 1H, J = 8.4 Hz, ArH), 6.79 (CH, d, 1H, J = 8.1 Hz, ArH), 6.86 (NH_2, s, 2H,), 7.14–7.21 (ArH, m, 3H), 7.27–7.32 (ArH, m, 2H), 9.81 (OH,s, 1H); MS: *m/z* (Cal. $C_{16}H_{12}N_2O_2$) = 264.2786 $[M]^+$; *m/z* (Obs.) =

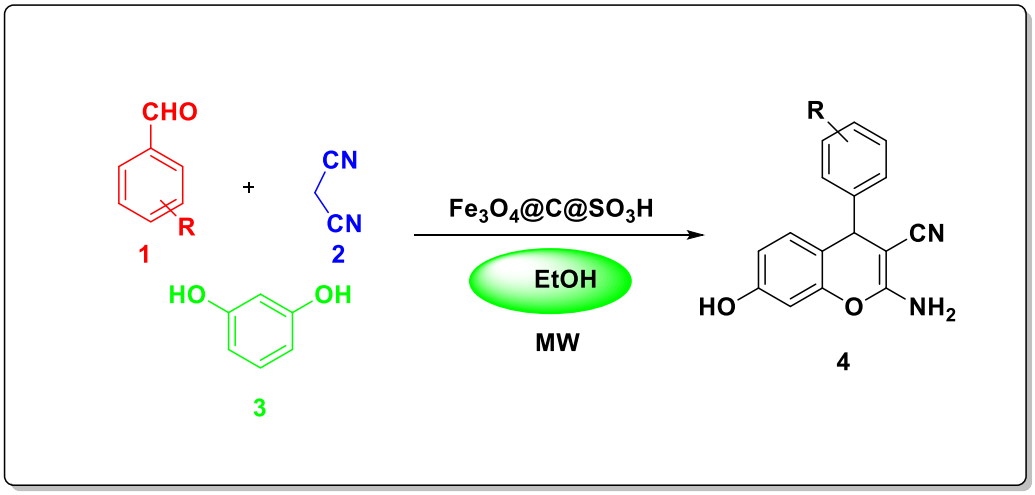

Scheme 1. General reaction of 2-amino-4*H*-chromene synthesis.

265.1500 $(M+H)^+$.

2-Amino-4-(2,3-dimethoxyphenyl)-7-hydroxy-4*H*-chromene-3-carbonitrile (4e): Solid; Yellow; FT-IR (cm^{-1}, KBr): 3466.24 (OH), 3340.57, 3248.18 (NH_2), 2925.15 (CH), 2191.40 (CN), 1641.72 (C=O); ^{1}H NMR (DMSO-d_6): (δ ppm) 2.10 (3H, s, CH_3), 2.45 (CH_3, s, 3H), 3.38 (CH, s, 1H), 4.92 (OH, s, 1H), 6.69 (CH, s, 1H), 6.80 (CH, s, 1H), 6.95 (C, s, 1H), 7.08–7.88 (Ar–H, m, 4H, $J = 6.6$), 8.01 (NH, s, 1H); LC-MS: *m/z* (Cal. $C_{18}H_{16}N_2O_4$) = 324.1254 $[M]^+$; *m/z* (Obs.) = 325.1989 $(M+H)^+$.

2-Amino-4-(4-(dimethylamino)phenyl)-7-hydroxy-4*H*-chromene-3-carbonitrile (4g): Solid; Yellow; FT-IR (cm^{-1}, KBr): 3809.28 (OH), 3490.36 (NH_2), 3327.80 (NH_2), 2938.75 (CH), 2212.06 (CN), 1567.28 (C=O); ^{1}H NMR (DMSO-d_6): (δ ppm) 2.45 (CH_3, s, 3H), 2.45 (CH_3, s, 3H), 4.46 (CH, s, 1H), 6.00 (CH, d, 1H), 6.10 (CH, s, 1H), 6.48–6.80 (Ar–H, m, 4H, $J = 6.4$), 7.78 (NH, s, 1H), 8.02 (OH, s, 1H); LC-MS: *m/z* (Cal. $C_{18}H_{17}N_3O_2$) = 307.1374 $[M]^+$; *m/z* (Obs.) = 308.2482 $(M+H)^+$.

3. Result and discussion

3.1 Preparation and characterization of the catalyst

The synthesis of Fe_3O_4@C–SO_3H by chemical method has been previously demonstrated for catalytic application in biodiesel production [66]. Hong et al. [67] employed the same catalyst in the hydrolysis of cellulose, and Zhang et al. [68] described the synthesis of *O*-2,3-unsaturated glycopyranosides[69]. Herein, we describe a green protocol synthesis of Fe_3O_4 NPs starting with $FeCl_3$ and $FeSO_4$ in the presence of agro-waste WELFSA as a catalytic solvent medium. The method developed was a chemical-free synthesis to give free-flowing magnetic Fe_3O_4 particles. Further, the mesoporous carbon was fabricated onto the surface of iron oxide, where it stabilized Fe_3O_4 against aggregation and also prevented its oxidation. It was grafted with SO_3H (Fe_3O_4@C–SO_3H), where it acts as a Bronsted acid. Lemon peel ash biomass waste was used as a carbon source for the synthesis of novel iron oxide carbon-based solid acid by a hydrothermal method. The surface functionalization increased the catalytic activity and stability by using lemon peel ash carbon followed by sulphuric acid (H_2SO_4) to give Fe_3O_4@C–SO_3H (Fig. 1). Fe_3O_4@C–SO_3H catalyst was characterized by various analytical techniques such as SEM-EDX, XRD, FT-IR, VSM, TGA, and XRF. The amorphous nature of the carbon shell on Fe_3O_4 was confirmed by the XRD pattern. The pattern for Fe_3O_4, Fe_3O_4@C, and Fe_3O_4@C–SO_3H in the wavelength range 400–4000 cm^{-1} is appended in (Fig. 2).

The presence of a strong absorption peak at 599 cm^{-1} is due to the presence of iron oxide of the Fe–O stretching vibration of the tetrahedral and C=C site of the spinel structure. The strong absorption band at 1635 cm^{-1} is due to the OH bending of physically held water molecules. The strong peak at 3400 cm^{-1} is due to the O–H stretching of water adsorbed on the surface of Fe_3O_4 (Fig. 2a). The weak bands at 866 and 1067 cm^{-1} are due to the C–O stretching of the surface carbon layer (Fig. 2b). The prominent peak at 3500 cm^{-1} is due to the surface –OH stretching of the –SO_3H, and 1117 cm^{-1} & 1151 cm^{-1} due to SO_2 symmetric and asymmetric stretching, respectively (Fig. 2c). The XRD pattern of the prepared MNPs are appended in Fig. 3, which shows the surface functionalized magnetic catalyst with diffraction peaks at 31.4, 36.7, 44.3, 52.5, 58.6 and 63.8, which are attributed to the (221), (310), (401), (421), (510) and (441) planes of Fe_3O_4, respectively (JCPDS No. 39-1346). These peaks indicate that the magnetic nature of Fe_3O_4 is kept in solid acid. This further confirms the sulfonation fabrication is not affected by the magnetic cores. For the amorphous carbonaceous shell, the XRD pattern shows many glitches in the baseline and the broad diffraction peak. The XRD pattern was collected for Fe_3O_4 from 0 to 60 degrees. Peaks at 21.02, 30.04, 35.66, 42.97, and 53.19 degrees are due to Fe of Fe_3O_4, and the peak at 23.23 degrees is due to the carbon layer present on the Fe_3O_4@C. The extra peak at 25.45 degrees is due to the SO_3H functionalization corresponding to Fe_3O_4 and Fe_3O_4@C (Fig. 3) [66–69].

Further, FE-SEM was recorded to check surface morphology and elements present in the prepared iron oxide derivative. The Fe_3O_4 showed fine particle size distribution ranging from 73–117 nm (determined by use of the Scherrer

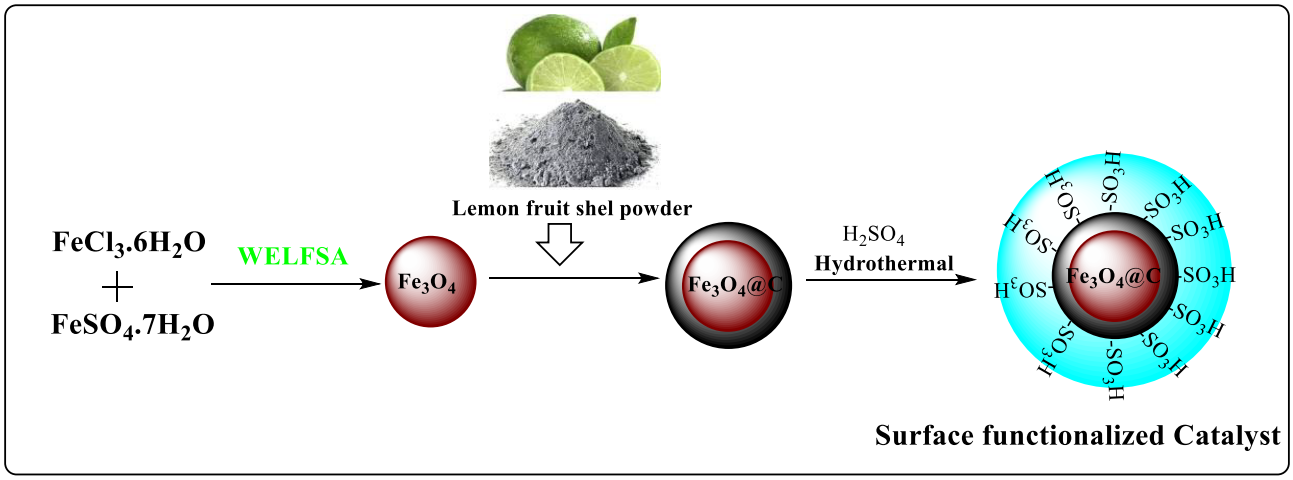

Figure 1. Pictorial representation of Fe_3O_4@C–SO_3H preparation.

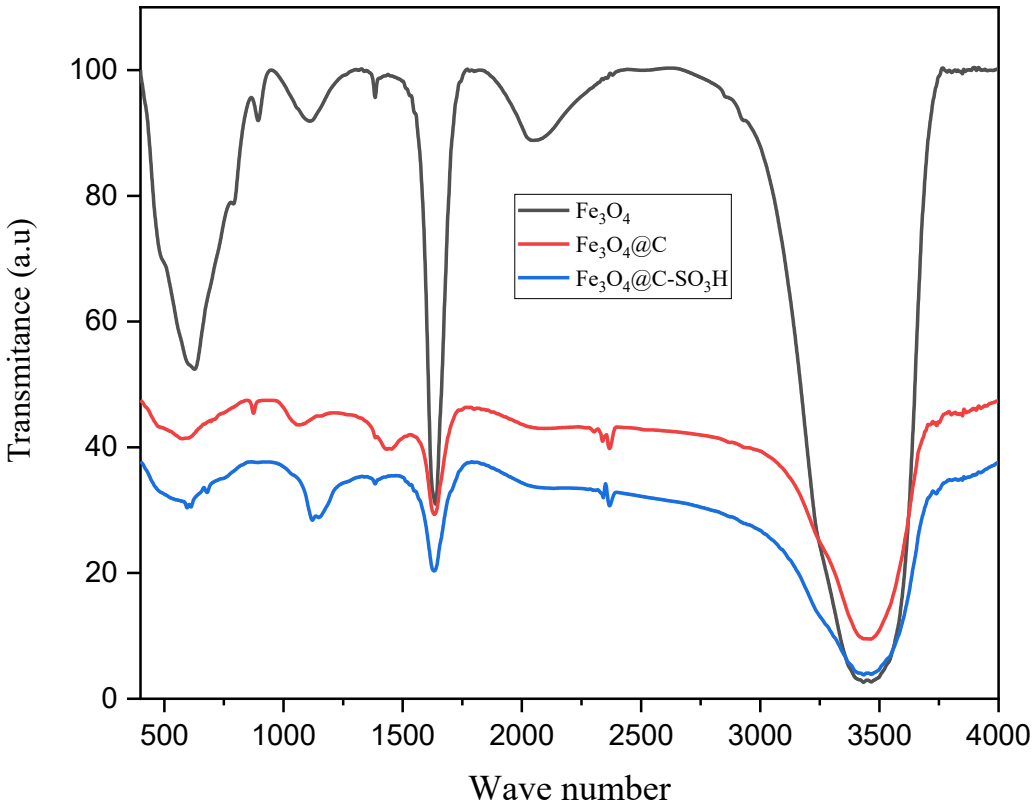

Figure 2. FT-IR Spectra of: a) Fe_3O_4, b) Fe_3O_4@C, and c) Fe_3O_4@C–SO_3H.

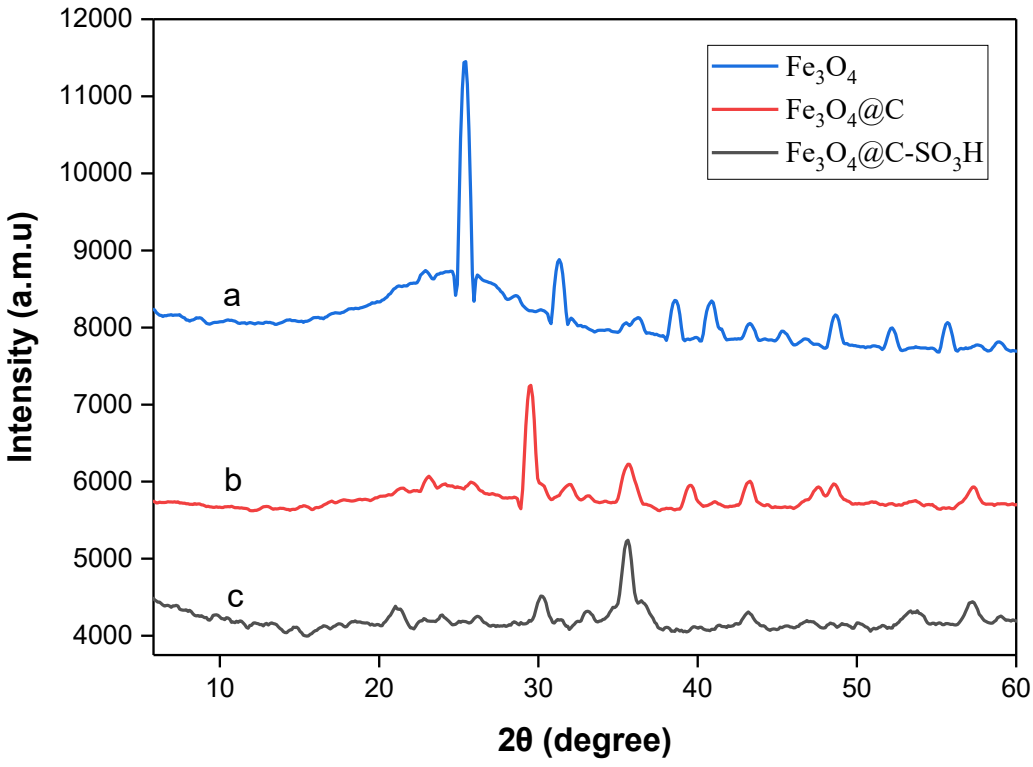

Figure 3. XRD Pattern of a) Fe_3O_4, b) Fe_3O_4@C, and c) Fe_3O_4@C–SO_3H.

equation) (Fig. 4a), with the presence of Fe as a major element. After surface modification with lemon fruit shell ash, the formation of carbon coating on Fe_3O_4 with a cavity was observed (Fig. 4b). The distribution of the carbon on the surface of the Fe_3O_4 was clearly observed by the elemental mapping (Fig. 4f). Further on carbon functionalized by the $-SO_3H$, the cavities with neatly formed small grove layered structures were observed (Fig. 4c, inset Fig. 4d). The elements present in a) Fe_3O_4, b) Fe_3O_4@C, and c)Fe_3O_4@C$-SO_3H$ were confirmed by EDS. The Fe peak was prominent in all EDS spectra along with the Au peak due to the gold-sputtered sample. After the surface modification by lemon fruit shell ash, new peaks in the spectra at 0.1 and 3.9, due to the C and Ca present in the ash, respectively, were observed (Fig. 5a). To increase the catalytic activity of the prepared material, it was further functionalized with $-SO_3H$ on carbon layer. Due to this, a new peak was observed around 2.9 for sulfur, and the remaining peaks observed were consistent for C, Fe, Au, and Ca (Fig. 5b & 5c). The correlation study of all these analytical techniques revealed the successful formation of the Fe_3O_4@C$-SO_3H$ material. The thermal stability of the surface of the functionalized catalyst was analyzed by TG-DTA. The thermogravimetric analysis was performed at

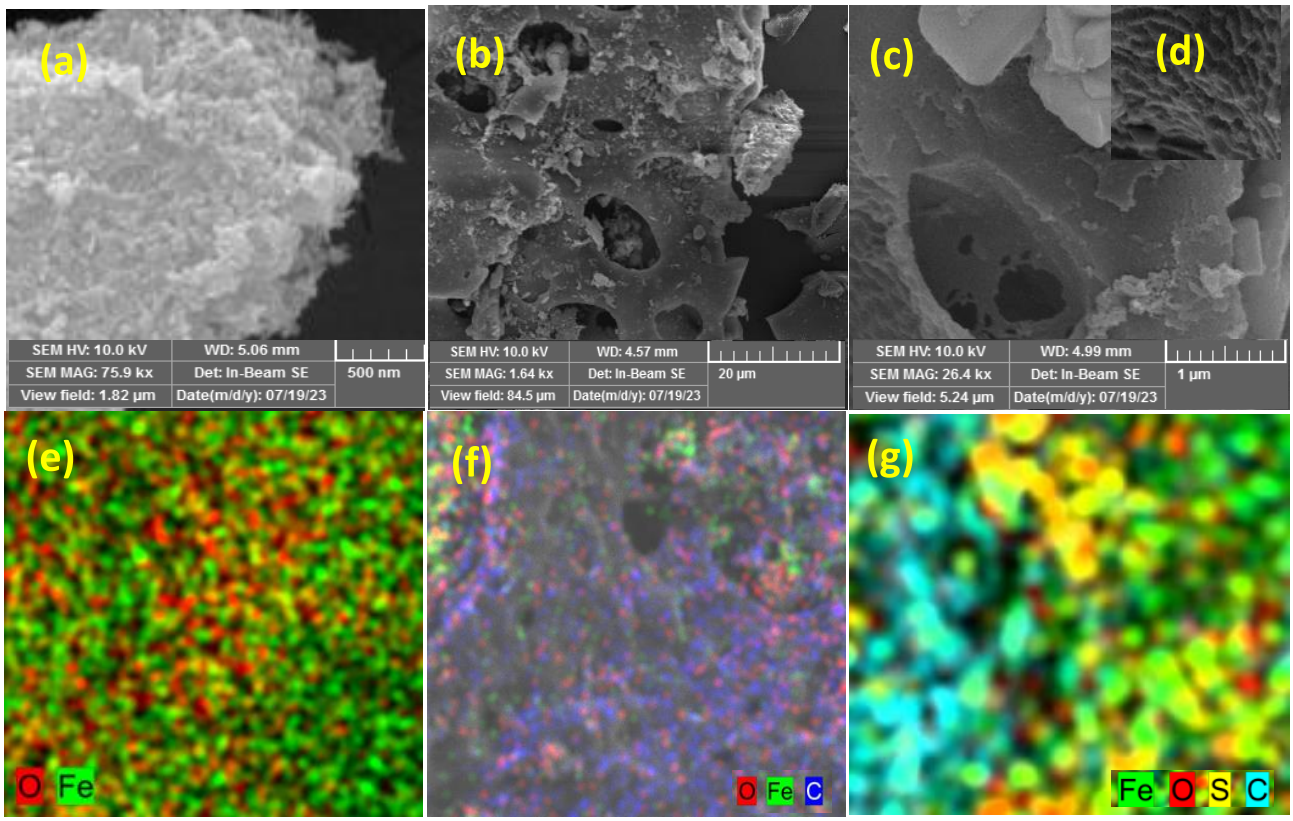

Figure 4. Comparative SEM image of: a) Crystaline Fe_3O_4 particles, b) Surface modified with carbon afforded porous Fe_3O_4@C, and c) Further functionalization with $-SO_3H$ gives groves on the top of the carbon layer; Elemental mapping of: e) Fe_3O_4, f) Fe_3O_4@C, and g) Fe_3O_4@C$-SO_3H$.

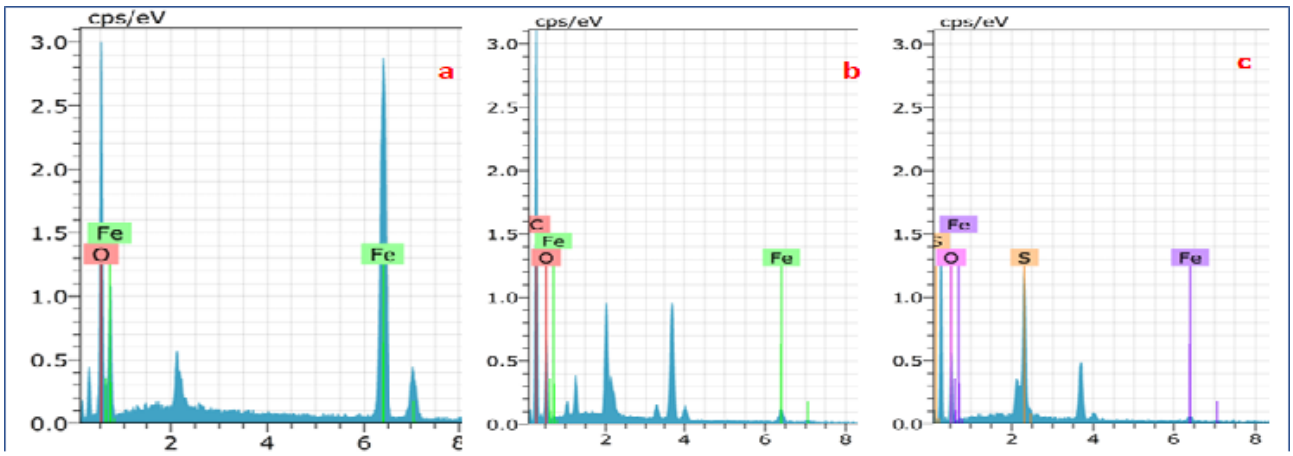

Figure 5. EDS Profile of: a) Fe_3O_4, b) Fe_3O_4@C, and c) Fe_3O_4@C$-SO_3H$.

room temperature under a nitrogen atmosphere up to 600 °C with a heating rate of 10 °C/min to know the decomposition behavior. The loss of physically bounded water led to a slight dip in the TG profile from 80 °C–140 °C. Later there was a slow decomposition induced due to the surface functionalized $-SO_3H$ layer, and the molecular weight decreased (Fig. 6). In DTA a broad curve was observed due to the physical change in the catalyst, and loss of physically bound water molecules. Further dip in the DTA profile represented physical change due to slow decomposition of the surface functionalized $-SO_3H$. The magnetic behavior of Fe_3O_4, Fe_3O_4@C, and Fe_3O_4@C$-SO_3H$ samples was examined by Vibrating Sample Magnetometer (VSM) with an applied field of 15 KG to −15 KG at room temperature Fig. 7, and its exposure to ferromagnetic nature. The detailed magnetic saturation (Ms), coercivity (Hc), and remnant magnetization (Mr) were estimated from the M-H plot outlined in Table 1. From Table 1, it is clearly indicated

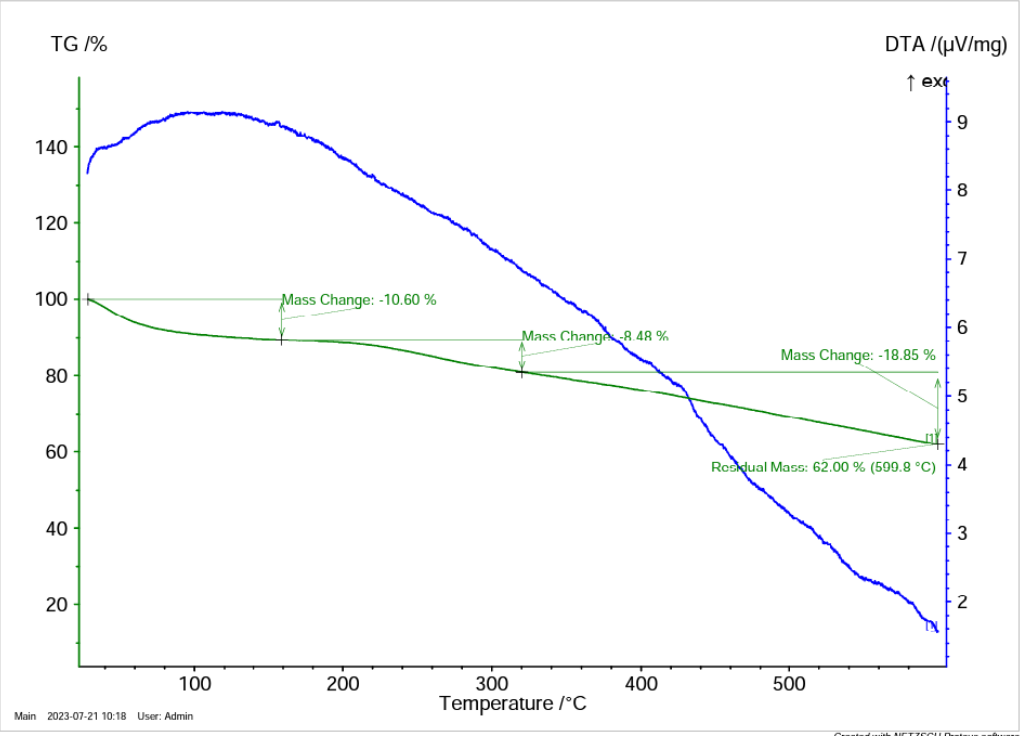

Figure 6. TG-DTA Profile of Fe_3O_4@C$-SO_3H$.

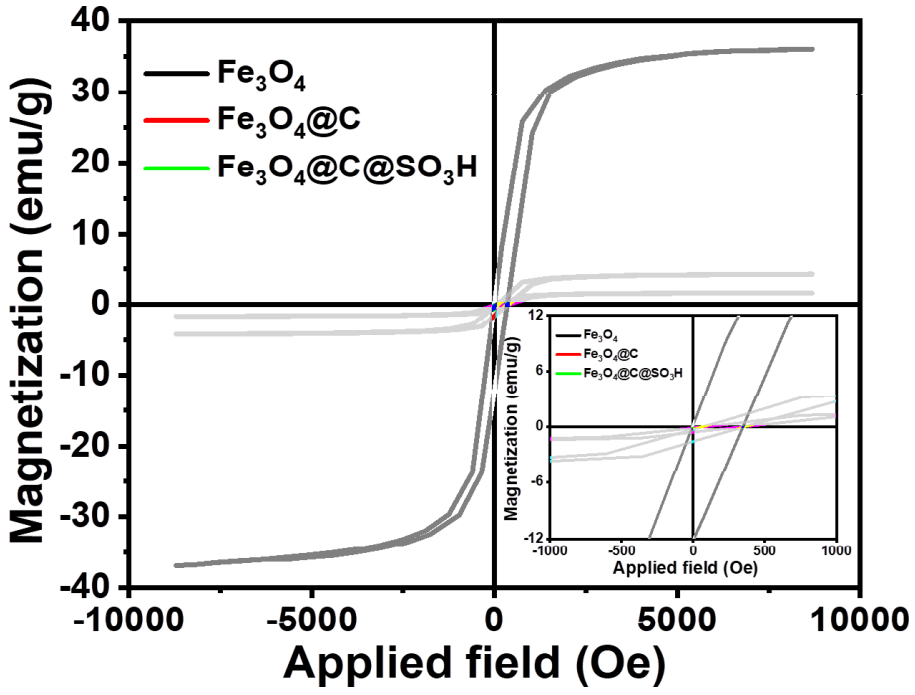

Figure 7. VSM Profile of Fe_3O_4, Fe_3O_4@C and Fe_3O_4@C$-SO_3H$.

Table 1. Data of magnetic saturation (Ms), remnant magnetization (Mr), coercivity (Hc), and magnetic susceptibility (X).

Sample	Ms (emu/g)	Mr (emu/g)	Hc (Oe)	X (emu/g · Oe)
Fe_3O_4	36.11	0.23	347.03	0.00415
Fe_3O_4@C	4.24	0.12	349.59	0.000487
Fe_3O_4@C–SO_3H	1.63	0.06	360.53	0.000187

that for pure Fe_3O_4, the Ms values are higher, and further substitution with carbon and SO_3H significantly reduces up to 40.17 emu/g. This suggests that, for higher dopant magnetic saturation decreases with increasing coercivity from 5.04 G to 6.85 G. Such nature points out that the hardness of the magnet slowly increases with a substituent. Observation of variation in magnetic behavior implies that it acts as a catalyst in the reaction. The magnetic properties of the derived sample were examined by VSM at room temperature with an applied field of −1 T to +1 T. The results from magnetic properties, including Magnetic saturation (Ms), remnant magnetization (Mr), coercivity (Hc), and magnetic susceptibility (X), were estimated and summarized in Table 1. Ms significantly changes from 36.11 to 1.63 emu/g. Such typical nature was observed because carbon and sulfonic acid, which were not magnetic in nature eventually showed certain magnetic saturation because of Fe^{3+} ions being replaced with carbon and sulfonic acid and creating free Fe^{2+} ions. The same was supported by Mr and Hc values evaluated in Table 1. We also cross-examined their magnetic susceptibility for each carbon and sulfonic acid blend, which was also strongly evidenced by the reduced magnetic properties as described in Table 1.

The application of this novel prepared heterogeneous catalyst (Fe_3O_4@C–SO_3H) was explored by demonstrating synthesis of 2-amino-4*H*-chromene derivatives by the reaction of aromatic aldehyde (1), malononitrile (2) and resorcinol (3) in 1 mmol scale and 25 mg of the catalyst as a model reaction in 2 mL of EtOH at room temperature stirring condition (Scheme 1). After 1 h stirring, solid product separation was noticed in the reaction vessel (TLC monitored). It was filtered, washed with dd water, and gave a low yield of the product. To accelerate the reaction, the model reaction was subjected to microwave irradiation. Surprisingly, under MW irradiation, the reaction was faster, and yield isolation was improved. In order to optimize the reaction, the model reaction was carried out with a series of different amounts of catalyst starting from 0 and followed by 5, 20, 25, and 30 mg of the catalyst under microwave irradiation at 300 W power, and the results are tabulated in Table 2. The experimental data revealed that the quantity of catalyst starting from 5–25 mg gave a gradual increase of the product yield isolation (entries 2–5, Table 2). Further increase of the quantity to 30 mg resulted in no change in the product isolation in 4 min microwave irradiation. This optimization reaction revealed that, for 1 mmol scale reaction (entry 5, Table 2) 25 mg of Fe_3O_4@C–SO_3H catalysts required 4 min MW irradiation time, gave highest yield of the product. Furthermore, to fix the microwave power, 300 W was found to be suitable for this reaction in terms of reaction acceleration and high product yield isolation.

To determine the optimum MW power required for the reaction, the model reaction was carried out at different MW power (entries 4–7, Table 3). The experimental data revealed that a decrease of the MW power to 100 W and 180 W leads to longer reaction time and decreased yield isolation (entries 4 & 5, Table 3). On the other hand, an increase in MW power above 300 W did not increase any product yield or decrease the reaction time. Thus, the presently developed approach demonstrated the faster, cleaner, and

Table 2. Optimization of the volume of catalyst in a model reaction[a].

Entry	Substrate in mmol	Catalyst in mmol	Quantity of catalyst (mg)	Time (min)	Isolated Yield (%)
1	1	0	0	4	Nill
2	1	0.015	5	4	25
3	1	0.031	10	4	32
4	1	0.046	20	4	68
5	1	0.077	25	4	91
6	1	0.092	30	4	91

a) Aldehyde (1 mmol), malononitrile (1 mmol), resorcinol (1 mmol), 25 mg of Fe_3O_4@C–SO_3H catalysts, microwave irradiation at 300 W power. The reaction completion was monitored by TLC, the catalyst was separated by a strong magnet, and the product was isolated.

Table 3. Effect of optimization of reaction rate and microwave power on reaction rate.

Entry	Methods	Power (W)	Time (min)	Isolated Yield (%)
1	Stirring@rt	–	60	65
2	Grindstone@rt	–	25	52
3	Ultrasound@rt	–	65	68
4	MWI	100	5	62
5	MWI	180	5	79
6	MWI	300	4	91
7	MWI	450	5	88

more efficient synthesis of 2-amino-4*H*-chromene using Fe_3O_4@C–SO_3H. Further, to compare the other methods available in the laboratory, the model reaction was performed using grindstone, ultrasound, and room temperature stirring methods. All these three methods gave poor product isolation with longer reaction time, and the observed experimental data is appended in Table 3, entries 1–3.

The diversity and tolerance of the developed protocol on substituents was checked by reaction of various substituents present on the aromatic aldehyde containing electron-withdrawing (EWG) and electron-donating group (EDG). It was observed that, the substituents containing EWG and EDG on aldehyde did not give any measurable effect on the rate of the reaction (Table 4).

3.2 Antimicrobial activities evaluation

The antimicrobial activities of some selected synthesized 2-amino-4*H*-chromene derivatives (4a, 4e, and 4g) were evaluated by standard disc diffusion method at the Clinical and Laboratory Standards Institute [70]. The antimicrobial inhibition assay was carried out *in vitro* using agar media at 37 °C incubation. The compounds (4a, 4e, and 4g) showed comparable activity tested against bacteria and fungi. The derivatives 4e and 4g showed activity against *Escherichia coli* and *Bacillus subtlis*, and the derivatives (4a, 4e, and 4g) showed activity against *Candida albicans*. 4a inhibited *Aspergillus niger*, while the other compounds showed less activity. The detailed evaluation of the antibacterial and antifungal activities of the compounds examined is tabulated in Table 5, where R represents the resistance.

3.3 Reusability of catalysts

Synthesis of 2-amino-4*H*-chromene from benzaldehyde, malononitrile, and resorcinol in the presence of the catalyst under optimized reaction conditions in a model reaction was performed. After the completion of the reaction, ethyl acetate was added to the reaction mixture, and the catalyst was separated by an external magnet. The separated catalyst was washed with dd water and ethanol twice, dried under vacuum at 80 for 5 h, and then reused for the consecutive cycles. The efficiency of the catalyst was observed up to four cycles without any significant loss in its activity, but in the fifth cycle, a comparatively low yield was isolated, as depicted in Fig. 8. Due to the chemisorption of certain species

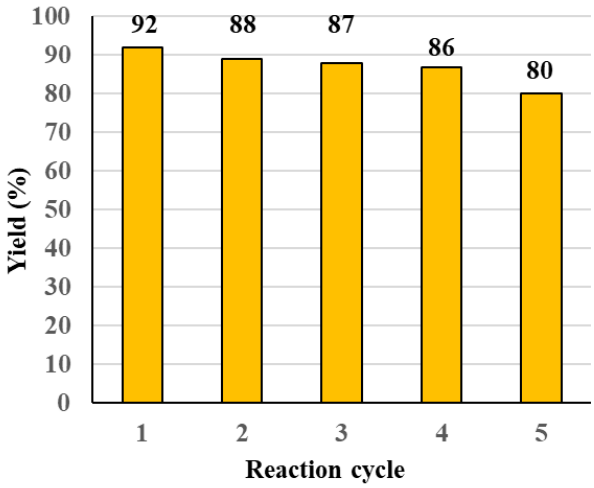

Figure 8. Reusability of the catalysts.

on the active sites and the vapor compound formation and/or leaching accompanied by molecular transport from the catalyst surface, it leads to a decrease in the catalytic activity after certain cycles (Fig. **??** and **??**). The TON of catalyst calculated with the no of mmol of the reactant with catalyst used to isolate 91 % of product yield was 12.98 sec^{-1}.

3.4 Comparison of the reported protocol with the present method

In this paper, we have compared the advantages of this developed method with selected reported procedures for the synthesis of chromene derivatives (Table 6). The reported methods (Table 6, serial no. 3, 6, 8, 9, 12) employed hazardous solvents and required a long reaction time for the chromene derivative synthesis. Overall, several methods reported in Table 6 used expensive catalysts, harsh reaction conditions, solvents harmful to the environment, and long reaction times, as well as low-yield product isolation. All these reported methods inspired us to develop an eco-friendly, recyclable, inexpensive approach for chromene scaffold synthesis.

The present developed protocol will reduce the effort in the separation of the catalyst from the reaction mixture; the agrowaste-derived carbon powder makes the shell on the nanoparticles very effective compared to other catalysts

Table 4. Substrate scope and physical parameters of 2-amino-4*H*-chromene.

Entry	Benzaldehyde	Product	Time (min)	Yield (%)	m.p. (°C)	
					Obs.	Rep.
1	H	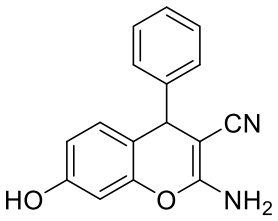 **4a**	4	94	233–235	233–235 [65]
2	4-OCH_3	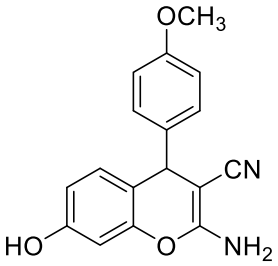 **4b**	4	90	110–112	112–113 [65]
3	4-CH_3	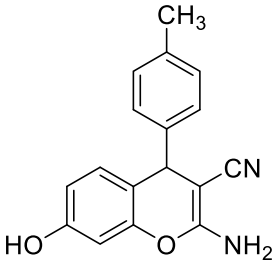 **4c**	5	88	183–185	184–186 [65]
4	4-Cl	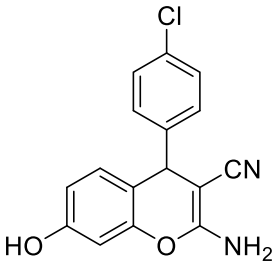 **4d**	4	91	160–161	162–163 [71]
5	2,3-OCH_3	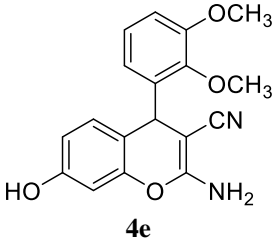 **4e**	4	89	184–186	New

Continued on next page

Table 4. Substrate scope and physical parameters of 2-amino-4*H*-chromene. (Continued)

Entry	Benzaldehyde	Product	Time (min)	Yield (%)	m.p. (°C)	
					Obs.	Rep.
6	4-OH	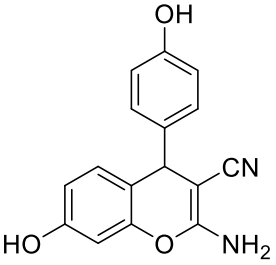 **4f**	5	90	247–249	247–249 [72]
7	4-N(CH_3)$_2$	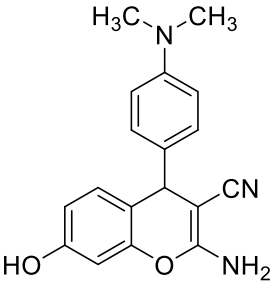 **4g**	4	90	206–207	New
8	3-NO_2	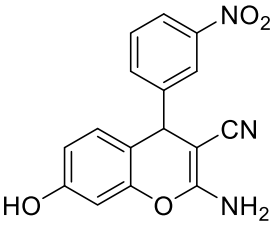 **4h**	4	90	171–172	170–171 [72]
9	4-CN	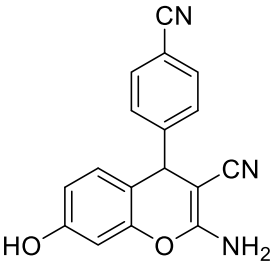 **4i**	4	87	179–181	180–182 [72]
10	4-Br	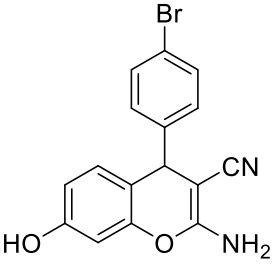 **4j**	4	86	186–188	185–187 [73]

Table 5. Antimicrobial activity of the 2-amino-4*H*-chromene derivatives.

	Organisms	Comp.	75 µL/mL	50 µL/mL	25 µL/mL	10 µL/mL	5 µL/mL
Antibacterial activity	*Escherichia coli*	4a	15 mm	R	R	R	R
		4e	10 mm	10 mm	R	R	R
		4g	10 mm	10 mm	R	R	R
	Ciprofloxacin		–	–	–	–	25 mm
	Bacillus subtilis	4a	18 mm	R	20 mm	R	R
		4e	20 mm	15 mm	12 mm	R	R
		4g	12 mm	18 mm	R	R	R
	Ciprofloxacin		–	–	–	30 mm	35 mm
	Pseudomonas	4a	12 mm	R	R	R	R
		4e	18 mm	15 mm	R	R	R
		4g	10 mm	15 mm	R	R	R
	Ciprofloxacin		–	–	45 mm	–	–
Antifungal activity	*Candida albicans*	4a	12 mm	10 mm	R	R	R
		4e	20 mm	15 mm	R	R	R
		4g	18 mm	15 mm	13 mm	R	R
	Fluconazole		–	–	30 mm	–	–
	Aspergillus niger	4a	10 mm	15 mm	10 mm	R	R
		4e	13 mm	12 mm	R	R	R
		4g	15 mm	18 mm	R	R	R
	Fluconazole		–	–	23 mm	–	–

Table 6. Comparison of reported with the present method.

Entry	Catalyst	Condition	Time (min)	Yield (%)	[Ref]
1	Nanocrystalline MgO	Rt	180	62	[74]
2	MNPs-Fe_3O_4/PCL–	80 °C/EtOAc	45	94	[75]
3	[bmim][BF_4]	Nill	240	84	[76]
4	t-ZrO_2 NPs	80 °C/H_2O	38	89	[77]
5	ZnO NPs	Reflux/EtOH	10	80	[78]
6	KF/Al_2O_3	rt/DMF	80–100	81	[79]
7	MNPs@Cu	90 °C/Solvent	8	95	[80]
8	Rochella salt	Reflux/EtOH	120–180	90	[54]
9	Triazine-based porous organic polymer	Solvent-free	300–360	87	[55]
10	Magnetic UiO-66 functionalized with 4,4′-diamino-2,2′-stilbened isulfonic	H_2O:EtOH (5:1)	360	73	[81]
11	Glycine	Hexane, DCM, DMF/EtOH	60	94	[82]
12	Cetyltrimethylammonium bromide (CTABr)	Solvent-free	300–480	60	[83]
13	Ionic liquid ([bmim]-OH)	Solvent-free	15–30	85	[84]
14	NaBr	EtOH	60–80	58	[56]
15	Fe_3O_4@C–SO_3H	MW/EtOH	4	90	This work

developed. Microwave irradiation adds another advantage, in which the energy synergistically aids in the increased isolation of the product yield.

4. Conclusion

MCRs of aryl aldehyde, malononitrile, and resorcinol to give 2-amino-4*H*-chromene in a single step using green method catalyzed Fe_3O_4@C–SO_3H as a novel heterogeneous catalyst has been described. The advantage of this approach is that the agro-waste derived solvent media has been employed for the core shell iron oxide preparation. Further, its surface modification is achieved with lemon ash (after filtration of the extraction medium), which gives a dual functional advantage. The prepared novel catalyst is characterized by various techniques. The synthetic method described is rapid, simple isolation of the product by crystallization, eliminating the use of chromatographic purification, inexpensive, recyclability of the catalyst, and a green synthetic protocol for the synthesis of valuable heterocyclic compounds. All the synthesized compounds were characterized by FT-IR, ^{1}H- & ^{13}C-NMR and LC-MS. Further antimicrobial activities of the selected 2-amino-4*H*-chromene derivatives (4a, 4e, and 4g) were evaluated by a disc diffusion method, and these derivatives showed moderate activities compared to standard drugs used as reference.

Acknowledgment

The authors are thankful to the SERB-SURE, GOI (SUR/2022/002631) and RCUB (RCU-IDR-2022-23) for the financial support to Dr. KK.

Authors Contributions

All authors have contributed equally to prepare the paper.

Availability of Data and Materials

The data that support the findings of this study are available from the corresponding author upon reasonable request.

Conflict of Interests

The authors declare that they have no known competing financial interests or personal relationships that could have appeared to influence the work reported in this paper.

References

[1] J.R. Cabrero-Antonino, R. Adam, V. Papa, and M. Beller. *Nat. Commun.*, **11**(2020):3893. DOI: https://doi.org/10.1038/s41467-020-17588-5.

[2] F. Poovan, V.G. Chandrashekhar, K. Natte, and R.V. Jagadeesh. *Catal. Sci. Technol.*, **12**(2022):6623–6649. DOI: https://doi.org/10.1039/D2CY00232A.

[3] C.M. Hendrich, K. Sekine, T. Koshikawa, K. Tanaka, A. Stephen, and K. Hashmi. *Chem. Rev.*, **121**(2020):9113–9163. DOI: https://doi.org/10.1021/acs.chemrev.0c00824.

[4] N.M. Sabry, H.M. Mohamed, E.S.A.E.H. Khattab, S.S. Motlaq, and A.M. El-Agrody. *Eur. J. Med. Chem.*, **2**(2011):765–772. DOI: https://doi.org/10.1016/j.ejmech.2010.12.015.

[5] S.R. Kolla and Y.R. Lee. *Tetrahedron*, **1**(2012):226–237, . DOI: https://doi.org/10.1016/j.tet.2010.09.050.

[6] A. Khalafi-Nezhad, S. Sarikhani, E.S. Shahidzadeh, and F. Panahi. *Green Chem.*, **10**(2012):2876–2884. DOI: https://doi.org/10.1039/c2gc35765h.

[7] H. Adibi, R. Khodarahmi, K. Mansouri, M. Khaleghi, and S. Maghsoudi. *Pharmaceutical Sciences*, **19**(2013):23–30.

[8] P.P. Ghosh and A.R. Das. *J. Org. Chem.*, **12**(2013): 6170–6181. DOI: https://doi.org/10.1021/jo400763z.

[9] R. Mohammadi and M.Z. Kassaee. *J. Mol. Catal. A. Chem.*, **380**(2013):152–158. DOI: https://doi.org/10.1016/j.molcata.2013.09.027.

[10] G. Brahmachari and S. Laskar. *Polycycl. Aromat. Compd*, **8**(2014):873–888. DOI: https://doi.org/10.1515/9783110985313-001.

[11] M.A. Ghasemzadeh, M.H. Abdollahi-Basir, and M. Babaei. *Green Chem. Lett. Rev.*, **4**(2015):40–49. DOI: https://doi.org/10.1080/17518253.2015.1107139.

[12] A. Maleki, R. Ghalavand, and R. Firouzi Haji. *Appl. Organomet. Chem.*, **32**(2018):e3916, . DOI: https://doi.org/10.1002/aoc.3916.

[13] D. Elhamifar, Z. Ramazani, M. Norouzi, and R. Mirbagheri. *J. Colloid Interface Sci.*, **511**(2018):392–401. DOI: https://doi.org/10.1016/j.jcis.2017.10.013.

[14] A. Maleki and S. Azadegan. *Inorg. Nano-Met. Chem*, **6**(2017):917–924, . DOI: https://doi.org/10.1080/24701556.2019.1577258.

[15] A. Maleki and S. Azadegan. *J Inorg Organomet Polym Mater.*, **3**(2017):714–719, . DOI: https://doi.org/10.1007/s10904-017-0514-z.

[16] A. Maleki. *Ultrason. Sonochem.*, **40**(2018):460–464, . DOI: https://doi.org/10.1016/j.ultsonch.2017.07.020.

[17] A.-H. Lu, E.L. Salabas, and F. Schuth. *Angew. Chem., Int. Ed. Engl.*, **8**(2007):1222–1244, . DOI: https://doi.org/10.1002/anie.200602866.

[18] A.-H. Lu, W. Schmidt, N. Matoussevitch, H. Bonnemann, B. Spliethoff, B. Tesche, E. Bill, W. Kiefer, and F. Schuth. *Angew. Chem., Int. Ed. Engl.*, **33**(2004):4303–4306, . DOI: https://doi.org/10.1002/anie.200454222.

[19] S.C. Tsang, V. Caps, I. Paraskevas, D. Chadwick, and D. Thompsett. *Angew. Chem., Int. Ed. Engl.*, **42**(2004):5763–5767. DOI: https://doi.org/10.1002/anie.200460552.

[20] B. Maleki, H. Natheghi, R. Tayebee, H. Alinezhad, A. Amiri, S.A. Hossieni, and S.M.M. Nouri. *Polycycl. Aromat. Compd.*, **40**(2020):633–643, . DOI: https://doi.org/10.1080/10406638.2018.1469519.

[21] R. Firouzi-Haji and A. Maleki. *Chemistry Select*, **4**(2019):853–857. DOI: https://doi.org/10.1002/slct.201802608.

[22] A. Maleki and R. Firouzi-Haji. *Sci. Rep.*, **8**(2018): 17303. DOI: https://doi.org/10.1038/s41598-018-35676-x.

[23] A. Maleki. *RSC Adv.*, **109**(2014):64169–64173, . DOI: https://doi.org/10.1039/C4RA10856F.

[24] A. Maleki. *Tetrahedron*, **38**(2012):7827–7833, . DOI: https://doi.org/10.1016/j.tet.2012.07.034.

[25] A. Maleki. *Tetrahedron*, **16**(2013):2055–2059, . DOI: https://doi.org/10.1016/j.tetlet.2013.01.123.

[26] F. Dumitrache, I. Morjan, R. Alexandrescu, R.E. Morjan, I. Voicu, I. Sandu, I. Soare, M. Ploscaru, C. Fleaca, and V. Ciupina. *Diam. Relat. Mater.*, **2**(2004):362–370. DOI: https://doi.org/10.1016/j.diamond.2003.10.022.

[27] J. Zheng, Z.Q. Liu, X.S. Zhao, M. Liu, X. Liu, and W. Chu. *Nat. Nanotechnol.*, **16**(2012):165601. DOI: https://doi.org/10.1088/0957-4484/23/16/165601.

[28] S. Pagoti, D. Dutta, and J. Dash. *Adv. Synth. Catal.*, **355**(2013):3532–3538. DOI: https://doi.org/10.1002/adsc.201300624.

[29] P. Riente, J. Yadav, and M.A. Pericas. *Org. Lett.*, **14**(2012):3668–3671. DOI: https://doi.org/10.1021/ol301515d.

[30] M.Z. Kassaee, H. Masrouri, and F. Movahedi. *RSC Adv.*, **10**(2020):44946–44957, . DOI: https://doi.org/10.1039/d0ra09087e.

[31] M.Z. Kassaee, H. Masrouri, and H. Masrouri. *Appl. Catal.*, **395**(2011):28–33, . DOI: https://doi.org/10.1016/j.apcata.2011.01.018.

[32] M.M. Khafagy, A.H.F. Abd El-Wahab, F.A. Eid, and A.M. El-Agrody. *Il Farmaco*, **57**(2002):715–722. DOI: https://doi.org/10.1016/S0014-827X(02)01263-6.

[33] K. Hiramoto, A. Nasuhara, K. Michikoshi, K. Kato, and K. Kikugawa. *Mutat. Res.*, **395**(1997):47–56. DOI: https://doi.org/10.1016/S1383-5718(97)00141-1.

[34] M. Kidwai, S. Saxena, M.K. Khan, and S.S. Thukral. *Bioorganic Med. Chem. Lett.*, **15**(2005):4295–4298. DOI: https://doi.org/10.1016/j.bmcl.2005.06.041.

[35] A.G. Martinez and L.J. Marco. *Bioorg Med. Chem. Lett.*, **7**(1997):3165–3170. DOI: https://doi.org/10.1016/S0960.

[36] K.N. Cobley, H. Weston, J. Scicinski, A. Merritt, A. Whittington, P. Wyatt, N. Taylor, D. Green, R. Bethell, S. Madar, R.J. Fenton, P.J. Morley, T. Pateman, and A. Beresford. *J. Med. Chem.*, **41**(1998): 787–797. DOI: https://doi.org/10.1021/jm970374b.

[37] S.J. Mohr, M.A. Chirigos, F.S. Fuhrman, and J.W. Pryor. *Cancer Res.*, **35**(197):3750–3754. DOI: https://doi.org/10.1515/cse-2016-0002.

[38] W.O. Foye. *Principi Di Chemico Farmaceutic Piccin*, **416**(1991).

[39] E.C. Witte, P. Neubert, and A. Roesch. *Ger. Offen DE. Chem. Abstr.*, **104**(1986):2249–15.

[40] F.Y.F. Ren, B. Yang, and X.L. Liao. *Catal. Sci. Technol.*, **6**(2016):4283–4293. DOI: https://doi.org/10.1039/C5CY01888A.

[41] C.S. Konkoy, D.B. Fick, S.X. Cai, N.C. Lan, and J.F.W. Keana. *Chem. Abstr.*, **134**(2001):29313a.

[42] G.P. Ellis, A. Weissberger, and E.C. Taylor. *Chromeones*, **13**(1977). DOI: https://doi.org/10.37652/juaps.2007.15597.

[43] E.A.A. Hafez, M.H. Elnagdi, A.G.A. Elagamey, and F.M.A.A. El-Taweel. *Heterocycles*, **26**(1987): 903–907. DOI: https://doi.org/10.3987/R-1987-04-0903.

[44] Y. He, R. Hu, R. Tong, F. Li, J. Shi, and M. Zhang. *Molecules*, **19**(2014):19253–19268. DOI: https://doi.org/10.3390/molecules191219253.

[45] Wanzheng MA, A.G. Ebadi, M. Shahbazi Sabil, R. Javahershenas, and G. Jimenez. *RSC Adv.*, **9**(2019): 12801. DOI: https://doi.org/10.1039/c9ra01679a.

[46] A. Zhu, Q. Li, W. Feng, D. Fan, and L. Li. *Catal. Letters*, **151**(2021):720–733. DOI: https://doi.org/10.1007/s10562-020-03332-7.

[47] S.R. Kolla and Y.R. Lee. *Tetrahedron*, **67**(2011):8271–1, . DOI: https://doi.org/10.1016/j.tet.2011.08.086.

[48] F.O. Chahkamali, S. Sobhani, and J.M. Sansano. *Sci. Rep.*, **12**(2022):2867. DOI: https://doi.org/10.1038/s41598-022-06759-7.

[49] P. Singh, P. Yadav, A. Mishra, and S.K. Awasthi. *ACS Omega*, **5**(2020):4223–4232. DOI: https://doi.org/10.1021/acsomega.9b04117.

[50] X. Yu and Z. Zhou. *Phosphorus Sulfur Silicon Relat. Elem.*, **193**(2018):387–393. DOI: https://doi.org/10.1080/10426507.2018.1424161.

[51] I.B. Masesane and S.O. Mihigo. *Synth Commun.*, **45**(2015):1546–1551. DOI: https://doi.org/10.1080/00397911.2015.1031249.

[52] M.G. Dekamin, M. Eslami, and A. Maleki. *Tetrahedron*, **69**(2013):1074–1085. DOI: https://doi.org/10.1016/j.tet.2012.11.068.

[53] S. Gupta, R. Banu, C. Ameta, R. Ameta, and P.B. Punjabi. *Top. Curr. Chem.*, **13**(2019):377. DOI: https://doi.org/10.1007/s41061-019-0238-3.

[54] T. Jin, A. Wang, J. Zhang, F. Zhang, and T. Li. *Chinese. J. Org. Chem.*, **24**(2004):1598–1600, .

[55] S.K. Kundu and A. Bhaumik. *RSC Adv.*, **5**(2015):32730–32739. DOI: https://doi.org/10.1039/C5RA00951K.

[56] S. Makarem, A.A. Mohammadi, and A.R. Fakhari. *Tetrahedron Lett.*, **49**(2008):7194–7196. DOI: https://doi.org/10.1016/j.tetlet.2008.10.006.

[57] S.K. Kundu, J. Mondal, and A. Bhaumik. *Dalton Trans.*, **42**(2013):10515–10524. DOI: https://doi.org/10.1039/C3DT50947H.

[58] R. Eivazzadeh Keihan, S. Bahrami, M.G. Gorab, Z. Sadat, and A. Maleki. *Scientific Reports*, **12**(2022). DOI: https://doi.org/10.1038/s41598-022-14844-0.

[59] S.L. Zhenga and L. Chen. *Org. Biomol. Chem.*, **19**(2021):10530. DOI: https://doi.org/10.1039/d1ob01906f.

[60] R. Heydari, R. Shahraki, M. Hossaini, and A. Mansouri. *Res Chem Intermed*, **43**(2017):4611–4622. DOI: https://doi.org/10.1007/s11164-017-2900-0.

[61] P. Sharma, M. Gupta, R. Kant, and V.K. Gupta. *RSC Adv.*, **6**(2016):32052–32059. DOI: https://doi.org/10.1039/C6RA06523F.

[62] R.L. Magar, P.B. Thorat, V.B. Jadhav, S.U. Tekale, S.A. Dake, B.R. Patil, and R.P. Pawar. *J. Mol. Catal. Chemica.*, **374**(2013):118–124. DOI: https://doi.org/10.1016/j.molcata.2013.03.022.

[63] K.R. Desale, K.P. Nandre, and S.L. Patil. *Org. Commun.*, **5**(2012):179–185.

[64] C. Gonzalez-Fernandez, J. Gómez-Pastora, E. Bringas, M. Zborowski, J.J. Chalmers, and I. Ortiz. *Ind. Eng. Chem. Res.*, **60**(2021):16780–16790. DOI: https://doi.org/10.1021/acs.iecr.1c03474.

[65] K. Kantharaju and S.Y. Khatavi. *Chemistry Select*, **18**(2018):5016–5024. DOI: https://doi.org/10.1002/slct.201800096.

[66] N. Yadav, G. Yadav, and Md. Ahmaruzzaman. *Sci. Rep.*, **13**(2023):9074. DOI: https://doi.org/10.1038/s41598-023-36380-1.

[67] C. Zhang, H. Wang, F. Liu, L. Wang, and H. He. *Cellulose*, **20**(2013):127–134. DOI: https://doi.org/10.1007/s10570-012-9839-5.

[68] G. Sun, S. Qiu, Z. Ding, H. Chen, J. Zhou, Z. Wang, and J. Zhang. *Synlett*, **28**(2016):347–350. DOI: https://doi.org/10.1055/s-0036-1588891.

[69] F. Kalantari, H. Esmailipour, H. Ahankar, A. Ramazani, H. Aghahosseini, O. Kaszubowski, and K. Slepokura. *ACS Omega*, **8**(2023):25780–25798. DOI: https://doi.org/10.1021/acsomega.3c01068.

[70] P.B. Hiremath and K. Kantharaju. *Curr. Microw. Chem.*, **1**(2019):30–43, . DOI: https://doi.org/10.2174/2213335606666190820091029.

[71] S. Shinde, S. Damate, S. Morbale, M. Patil, and S.S. Patil. *RSC Advances*, **12**(2017):7315–7328. DOI: https://doi.org/10.1039/C6RA28779D.

[72] M. Sarmah, A. Dewan, A.J. Thakur, and U. Bora. *Chemistry Select*, **24**(2017):7091–7095. DOI: https://doi.org/10.1002/slct.201701057.

[73] P.B. Hiremath and K. Kantharaju. *Chemistry Select*, **6**(2020):1896–1906, . DOI: https://doi.org/10.1080/10406638.2020.1830129.

[74] J. Safari, Z. Zarnegar, and M. Heydarian. *J. Taibah Univ. Sci.*, **7**(2013):17–25. DOI: https://doi.org/10.1016/j.jtusci.2013.03.001.

[75] M. Keshavarz, M. Abdoli-Senejani, S.F. Hojati, and S. Askari. *Reac Kinet Mech Cat*, **124**(2018):757–766. DOI: https://doi.org/10.1007/s11144-018-1361-9.

[76] X. Fan, X. Hu, X. Zhang, and J. Wang. *Aust. J. Chem.*, **57**(2004):1067–1071. DOI: https://doi.org/10.1071/CH04060.

[77] A. Saha, S. Payra, and S. Banerjee. *RSC Adv.*, **5**(2015): 101664. DOI: https://doi.org/10.1039/c5ra19290k.

[78] S. Zavar. *Arab. J. Chem.*, **10**(2017):S67–S70. DOI: https://doi.org/10.1016/j.arabjc.2012.07.011.

[79] W. Xiang-Shan, S. Da-Qing, and T. Shu-Jiang. *Chinese J. Chem.*, **21**(2003):1114–1117.

[80] W. MA, A.G. Ebadi, M.S. Sabil, R. Javahershenas, and G. Jimenez. *RSC Adv.*, **9**(2019):12801–12812. DOI: https://doi.org/10.1039/c9ra01679a.

[81] M.R. Khodabakhshi and M.H. Baghersad. *Sci. Rep.*, **12**(2022):5531. DOI: https://doi.org/10.1038/s41598-022-09337-z.

[82] B. Datta and M.A. Pasha. *Ultrason Sonochem*, **19**(2012):725–728. DOI: https://doi.org/10.1016/j.ultsonch.2012.01.006.

[83] T.-S. Jin, J.-C. Xiao, S.-J. Wang, and T.-S. Li. *Ultrason Sonochem*, **11**(2004):393–397, . DOI: https://doi.org/10.1016/j.ultsonch.2003.10.002.

[84] N. Surneni, N.C. Barua, and B. Saikia. *Tetrahedron Lett.*, **25**(2016):2814–2817. DOI: https://doi.org/10.1016/j.tetlet.2016.05.048.